

# Theory of interconfigurational nonradiative transitions in transition-metal ions in solids and application to the $\text{Ti}^{3+}:\text{Al}_2\text{O}_3$ system

M. Grinberg

*Institute of Physics, Nicholas Copernicus University, PL 87-100 Torun, Poland*

A. Mandelis

*Photothermal and Optoelectronic Diagnostics Laboratory, Department of Mechanical Engineering, University of Toronto, Toronto, Canada M5S 1A4*

K. Fjeldsted

*Crystar Research Corporation, Victoria, British Columbia, Canada*

(Received 2 November 1992)

In this paper the nonradiative deexcitation of transition-metal ions in solids is discussed. It has been found that when the deexcitation of the system occurs due to the crossing of the configurational energies of ground and excited electronic manifolds (the internal conversion process) the system dynamics can be described by the perturbation method. Detailed investigation of two equivalent approaches, the adiabatic and the diabatic, shows that the diabatic attempt is usually more useful, since it allows the description of the vibronic problem in the harmonic-oscillator limit. The model has been successfully applied for describing the temperature quenching of  $\text{Ti}^{3+}:\text{sapphire}$  luminescence.

## I. INTRODUCTION

The effect of radiative relaxation of transition metals is usually diminished by the large temperature quenching of broadband emission. The simplest model describing this phenomenon has been proposed by Mott,<sup>1</sup> who related the nonradiative deexcitation processes to the crossover of the configuration-coordinate energy surfaces, describing the system in the excited and ground states. Thus the effect of thermal quenching of the fluorescence has been described by some adequate activation energy  $E_{\text{NR}}$ , related to the height of the crossing point over the minimum energy of the excited state, and the so-called "frequency factor"  $\tau_0^{-1}$ , related to the probability of a transition over the barrier. A more sophisticated approach has been proposed by Struck and Fonger,<sup>2,3</sup> who have been able to calculate the tunneling through the barrier as an effect proportional to the overlap integrals of the vibronic wave functions of the excited and ground manifolds, using the single-configuration-coordinate model. An important development in the approach of Struck and Fonger has been presented by Bartram *et al.*,<sup>4,5</sup> who assumed that the nonradiative transitions are related to the matrix elements of the nonadiabatic part of the Hamiltonian. Considering an arbitrary number of lattice vibrational modes, interacting (promoting modes) and noninteracting (accepting modes) with the electronic system, they could describe the nonradiative processes in a more accurate way, including the effects of Jahn-Teller-type distortions. One can find an excellent review of the models based on the configuration-coordinate scheme in Englman.<sup>6</sup>

Despite the theoretical efforts, our understanding of the processes of interconfigurational nonradiative deexcitation is still not complete. The main issue is the weak knowledge of the physical processes which cause the

internal conversion of the system from the excited to the ground electronic state. This is a reason why a large amount of experimental data concerning temperature fluorescence quenching (i.e., the fitted values of frequency factor as well as the activation energy in different ions and materials) cannot be properly interpreted. Especially the frequency factor, which according to the Mott model should be more or less a universal constant, changes its value from material to material and from ion to ion by 13 orders of magnitude [from  $6 \times 10^{-4} \text{ s}^{-1}$  for zirconate glasses<sup>7</sup> to  $10^{17} \text{ s}^{-1}$  for Ce-doped  $\text{YAl}_2\text{O}_3$  Ref. (8)]. Furthermore, for rather simple and relatively well-known systems such as ruby ( $\text{Al}_2\text{O}_3:\text{Cr}^{3+}$ ) Ref. (3) and sapphire ( $\text{Al}_2\text{O}_3:\text{Ti}^{3+}$ ),<sup>9</sup> calculations performed using the Struck-Fonger model evidently break down the Mott assumption concerning the universal frequency factor.

## II. GENERAL REMARKS AND ASSUMPTIONS: DIABATIC vs ADIABATIC APPROACH

To begin with, in order to discuss the processes responsible for interconfigurational nonradiative deexcitation, let us consider the simplest case, when the system can be described by two electronic manifolds (the ground and excited one) characterized by a large offset of the configurational energies. For simplicity, we may assume that the offset is the result of the interaction with fully symmetric lattice distortion, and so the above-mentioned manifolds can be presented in a one-dimensional configuration-coordinate diagram. This assumption is not obvious, and the model will be developed to consider an arbitrary number of modes involved and participating basis wave functions. The Hamiltonian can be presented in a perturbation formalism (Appendix), the adiabatic as well as in the diabatic approximation

$$H = H_0 + H' + H'' , \quad (1)$$

where  $H_0$  is the diagonal part of the Hamiltonian which gives the states related to each individual manifold.  $H'$  is a perturbation which mixes the states from different manifolds, and  $H''$  describes the interaction of the ion-ligand subsystem with the entire lattice. In both cases the eigenstates of  $H_0$  are given by Born-Oppenheimer wave functions of the type

$$\psi_v^m(q, Q) = \phi_v(q, Q) \lambda_v^m(Q) , \quad (2)$$

where  $\phi_v(q, Q)$  is the electronic part of the wave function and  $\lambda_v^m(Q)$  is the vibronic wave function.  $q$  and  $Q$  are the electronic and ionic (configuration-)coordinates, respectively. It is characteristic that it is usually possible to choose the diabatic basis so that the electronic wave function does not depend on  $Q$  (as in the case presented in the Appendix). Configuration-coordinate diagrams corresponding to  $H_0$  for a two-manifold system are presented in Fig. 1. One can see that for the diabatic basis there is no anticrossing behavior of the electronic manifolds [Fig. 1(b)], such as appears for the adiabatic basis [Fig. 1(a)]. The perturbation Hamiltonian  $H'$  depends on the basis, and for the adiabatic basis it is always the so-called nonadiabatic Hamiltonian which acts on the Born-Oppenheimer wave functions as follows:

$$H' \psi_v^m(q, Q) = -\frac{1}{2} \lambda_v^m(Q) \frac{d^2 \phi_v(q, Q)}{dQ^2} - \frac{d\phi_v(q, Q)}{dQ} \frac{d\lambda_v^m(Q)}{dQ} , \quad (3)$$

whereas for the diabatic basis it is a part of the electronic and/or the electron-lattice interaction Hamiltonian.

Since the information about the whole lattice is usually poor, the perturbation  $H''$  can be added in both cases in the same form, independent of the basis used for describing the ion-ligand subsystem. Since  $H_0$  is not the full Hamiltonian,  $H' + H''$  is nonzero, and the eigenstates of  $H_0$  are not the stationary states of the entire system (ion+ligands+lattice) or the subsystem (ion+ligands). This causes the nonradiative transitions, which yield the relaxation and internal conversion processes. One can recognize two types of such transitions. The first one is when the subsystem emitting phonons does not change the electronic manifold (intraconfiguration relaxation), and the second is when the manifold is changed (interconfigurational relaxation). The second process can

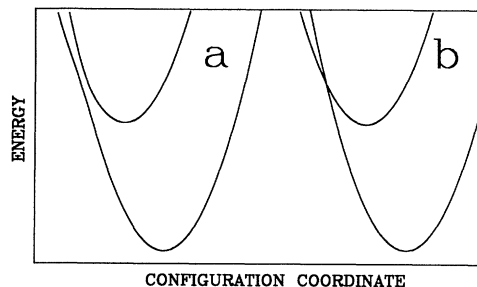


FIG. 1. Configuration-coordinate diagram for two electronic manifolds: (a) adiabatic limit; (b) diabatic limit. The diagram has been calculated assuming that the part of the Hamiltonian which mixes the manifolds does not depend on the configuration coordinate  $Q$ .

be divided into two steps: the internal conversion of the subsystem for the excited to the ground electronic manifold (via the vibronic degenerate states) and emission of phonons by intraconfiguration processes. It is obvious that the intraconfigurational processes take place due to the interaction of the subsystem with the entire lattice,  $H''$ , whereas the internal conversion takes place due to the subsystem perturbation Hamiltonian  $H'$ . Since the subsystem is usually converted to a very highly excited phonon state, the intraconfigurational transition rate is much larger than the internal-conversion rate. Therefore the internal conversion actually controls the nonradiative interconfigurational deexcitation.

The idea that internal-conversion processes can cause the nonradiative deexcitation has been proposed by Robinson and Frosch<sup>10</sup> for molecules. One can find a review on this subject in Ref. 11.

According to the above discussion, the interconfigurational transition probability can be calculated as the probability of internal conversion between excited and ground electronic manifolds. One can use the standard method and calculate this quantity as the probability of transition,  $W_{eg}^{nm}$ , related to the time-independent perturbation  $H'$ .<sup>12</sup>

$$W_{eg}^{nm} = (2\pi/\hbar) \delta(E_e^n - E_g^m) |T_{eg}^{nm}|^2 \rho(E_e^n) , \quad (4)$$

where  $\rho(E_e^n)$  is the density of states in the excited electronic manifold and  $\delta(E_e^n - E_g^m)$  is the Dirac delta function. The matrix  $T_{eg}^{nm}$  is related to  $H'$  as follows:

$$T_{eg}^{nm} = \langle\langle \psi_e^n | H' | \psi_g^m \rangle\rangle + \sum_{v,k} \frac{\langle\langle \psi_e^n | H' | \psi_v^k \rangle\rangle \langle\langle \psi_v^k | H' | \psi_g^m \rangle\rangle}{E_e^n - E_v^k} + \sum_{v',k'} \frac{\langle\langle \psi_e^n | H' | \psi_v^k \rangle\rangle \langle\langle \psi_v^k | H' | \psi_{v'}^{k'} \rangle\rangle \langle\langle \psi_{v'}^{k'} | H' | \psi_g^m \rangle\rangle}{(E_e^n - E_v^k)(E_e^n - E_{v'}^{k'})} + \dots , \quad (5)$$

where  $\langle\langle \dots \rangle\rangle$  indicates integration over the  $q$  and  $Q$  coordinates,  $v, v'$  are the electronic quantum numbers, and  $k, k'$  are vibronic quantum numbers.

It is easy to see that, although the adiabatic approach gives always the same perturbation Hamiltonian, the dia-

batic base is very useful for proceeding further even if sometimes some extra effort must be made to generate this basis. The main reason is that in the diabatic base we can get electronic wave functions that are not dependent on the vibronic (ionic) coordinate  $Q$ . A very important

consequence of this result is that the vibronic wave functions can be approximated by the harmonic-oscillator wave functions. If one operates in the framework of the adiabatic approach, all matrix elements of the nonadiabatic Hamiltonian depend on the particular dependence of the electronic wave function on  $Q$ . Also, because of the large anticrossing of the electronic manifolds, the vibronic wave functions cannot be approximated by the harmonic-oscillator wave functions. This casts doubt to all approximations made to simplify the procedure of calculations and to perform the qualitative analysis of the process. Thus, to obtain accurate  $T$ -matrix elements, one must calculate numerically the vibronic wave functions and perform inconvenient numerical integrations in  $Q$  space. In the diabatic approach, the problem is simpler. Here the perturbation Hamiltonian  $H'$  is a part of the electronic Hamiltonian or of an electron-phonon interaction Hamiltonian. In the former case, we have

$$H' = H'(q), \quad (6)$$

and in the latter case, the linear coupling gives

$$H' = \left[ \frac{dV(q, Q)}{dQ} \right] Q = H'(q)Q. \quad (7)$$

Using the diabatic wave function

$$\psi_v^m(q, Q) = \phi_v(q) \lambda_v^m(Q), \quad (8)$$

where  $\lambda_v^m(Q)$  is the harmonic-oscillator wave function, one obtains

$$\langle\langle \psi_v^m | H' | \psi_v^m \rangle\rangle = \langle \phi_v | H' | \phi_v \rangle F_{vv}^{m'm}, \quad (9)$$

where the overlap integral  $F_{vv}^{m'm}$  depends on  $H'$  and is

$$F_{vv}^{m'm} = \langle \lambda_v^m | \lambda_v^m \rangle \quad (10)$$

for  $H'$  given by Eq. (6) and

$$F_{vv}^{m'm} = \langle \lambda_v^m | Q | \lambda_v^m \rangle \quad (11)$$

for  $H'$  given by Eq. (7).

In both cases, however, since  $H'$  is given by off-diagonal matrix elements, when the subsystem is restricted to two electronic manifolds, the even-order components of sum (5) are zero. Moreover, since the overlap integrals are calculated for highly excited oscillator wave functions, the only important contribution comes from the first-order component of (5) (linear approximation). In this case the  $T$  matrix is given by

$$T_{eg}^{nm} = \langle \phi_e | H' | \phi_g \rangle F_{eg}^{nm}. \quad (12)$$

It should be noted that if  $\langle \phi_e | H' | \phi_g \rangle = 0$ , one must also consider other excited electronic states (higher excited states) of the system. In such a case, the internal-conversion probability is given by even-order components of (5), and considering only the most important, second-order, contribution, one obtains

$$T_{eg}^{nm} = \sum_{\substack{v, k \\ v \neq e, g}} \frac{\langle \phi_e | H' | \phi_v \rangle \langle \phi_v | \phi_g \rangle F_{ev}^{nk} F_{vg}^{km}}{E_e^n - E_v^k}. \quad (13)$$

### III. CALCULATIONS

#### A. Calculation of the frequency factor $\tau_0^{-1}$

To calculate the possible value of the transition probability, one can consider two one-dimensional harmonic oscillators as in Fig. 1(b). For this case the density of states in the excited energy manifold is constant,  $\rho(E_e^n) = (\hbar\omega)^{-1}$ , where  $\hbar\omega$  is the phonon energy. Thus, using Eq. (12), we obtain

$$W_{eg}^{nm} = (2\pi/\hbar)(\hbar\omega)^{-1} |\langle \phi_e | H' | \phi_g \rangle|^2 |F_{eg}^{nm}|^2 \times \delta(E_e^n - E_g^n). \quad (14)$$

Assuming that  $H'$  is a pure electronic Hamiltonian, this formula reproduces exactly the Struck-Fonger model.<sup>2</sup>

For the transition metals, the Hamiltonian which mixes the states belonging to different electronic configurations is usually the spin-orbit interaction Hamiltonian (e.g.,  ${}^4T_2$  and  ${}^4A_2$  states of  $\text{Cr}^{3+}$  or  ${}^2E$  and  ${}^2T_2$  states of  $\text{Ti}^{3+}$  in the octahedral field<sup>13</sup>). The importance of the spin-orbit coupling in the nonradiative processes has been mentioned by Sturge<sup>14</sup> for  $\text{KMgF}_3:\text{Co}^{2+}$ . To calculate the frequency factor, one can use a typical value of the spin-orbit matrix element  $H_{s.o.} = 50-500 \text{ cm}^{-1}$  and a typical value of phonon energy  $\hbar\omega = 250 \text{ cm}^{-1}$  and obtain

$$\tau_0^{-1} = (2\pi/\hbar)(\hbar\omega)^{-1} |\langle \phi_e | H' | \phi_g \rangle|^2 = (2\pi/\hbar) H_{s.o.}^2 / \hbar\omega = 10^{13} - 10^{14} \text{ s}^{-1}. \quad (15)$$

The situation is different when the symmetry allows the mixing of the electronic wave functions of the ground and excited states due to the interaction with the lattice distortion. In such a case, the matrix element of the electronic wave functions is given by

$$\langle \phi_e | H' | \phi_g \rangle = \langle \phi_e | dV(q, Q)/dQ | \phi_g \rangle = V_{eg}, \quad (16)$$

and  $F_{eg}^{nm}$  is given by Eq. (11).

One can assume in this case that the mixing may be quite effective; i.e.,  $V_{eg}$  may be on the order of the magnitude of

$$V_{ee} = \langle \phi_e | dV(q, Q)/dQ | \phi_e \rangle = (2S\hbar\omega)^{1/2}$$

(see the Appendix), where  $S$  is the Huang-Rhys factor, which describes the energy offset. On the other hand, considering that  $Q = 2^{-1/2}(a_e^\dagger + a_e)$ , where  $a_e^\dagger$  and  $a_e$  are the creation and annihilation phonon operators acting on the phonons in the excited state, one can approximate  $F_{eg}^{nm}$  by

$$F_{eg}^{nm} = (2n\hbar\omega)^{1/2} \langle \lambda_e^n | \lambda_g^m \rangle. \quad (17)$$

Since we are interested in the value of  $\tau_0^{-1}$  for  $n$  corresponding to activation energy  $E_{NR}$ , one can put  $n\hbar\omega = E_{NR}$  to obtain

$$\tau_0^{-1} = (2\pi/\hbar)(\hbar\omega)^{-1} |\langle \phi_e | H' | \phi_g \rangle|^2 = (2\pi/\hbar)(\hbar\omega)^{-1} 4S\hbar\omega E_{NR}. \quad (18)$$

Considering that  $S\hbar\omega$  is on the order of  $1000 \text{ cm}^{-1}$  and  $E_{NR}$  may even be a few times greater, one obtains  $\tau_0^{-1}$  on

the order of  $10^{16}-10^{17} \text{ s}^{-1}$ . One can see that in this case the Struck-Fonger model can work due to the approximation (17), however, with a much greater frequency factor. One should also consider the case when  $\langle \phi_e | H' | \phi_g \rangle = 0$ . Here the probability of the internal conversion should be calculated using the  $T$  matrix approximated by Eq. (13). For performing the estimation of  $\tau_0^{-1}$  in this case, one can assume that we have only one higher excited state  $\nu$  and that there is no offset between  $\nu$  and  $e$  electronic manifolds. Under these simplifications, since  $F_{ev}^{nk} = \delta_{nk}$  yields  $F_{ev}^{nk} F_{vg}^{km} = F_{eg}^{nm}$ , one can calculate the internal-conversion probability as follows:

$$W_{eg}^{nm} = (2\pi/\hbar) \delta(E_e^n - E_g^m) (\hbar\omega)^{-1} \times \frac{|\langle \phi_e | H' | \phi_\nu \rangle|^2 |\langle \phi_\nu | H' | \phi_g \rangle|^2}{(E_e - E_\nu)^2} |F_{eg}^{nm}|^2, \quad (19)$$

where the overlap integral  $F_{eg}^{nm}$  is given by Eq. (10).

Considering that the value of  $(E_g - E_\nu)$  is equal to a few thousand  $\text{cm}^{-1}$  and the electronic matrix elements are equal to  $\sim 100 \text{ cm}^{-1}$ , Eq. (19) yields  $\tau_0^{-1}$  on the order of  $10^9 \text{ s}^{-1}$  or even less, depending on the individual case, especially when the simplification of the absence of energy offset in the excited state is not valid.

It is interesting to mention that for all considered cases, for different types of interaction yielding internal-conversion processes, although very different values of the frequency factor have been obtained, the probability of a transition is always governed by the Struck-Fonger prediction. However, the model as proposed by Struck and Fonger<sup>2</sup> is strictly valid only in the case when  $H'$  is a pure electronic Hamiltonian (i.e., it does not depend on  $Q$ ). In other cases the formalism resulting from overlap integrals of vibronic wave functions can be reduced to the Struck-Fonger formula under some additional conditions, not always satisfied.

### B. Case of two- and three-dimensional local lattice modes

It usually happens that the electronic system of a transition-metal ion is coupled to not fully symmetrical lattice distortion. For the case of octahedral and tetrahedral coordination, we should consider two-dimensional distortion of  $E$  symmetry and three-dimensional distortion of  $T_1$  or  $T_2$  symmetry. To simplify the problem, let us assume that the static Jahn-Teller distortion splits the initially degenerate electronic manifold in such a way that, instead of single manifold, we have a few new manifolds with the same shape, but with the minima shifted to different points in the configurational space. Thus, independent of the resulting number of manifolds in the ground and excited states, we can consider the internal-conversion processes involving pairs of manifolds, one from the ground and one from the excited state, and thus summarize the effects. The diabatic basis allows the simplification of the problem, since each manifold can be described by a two- or three-dimensional harmonic oscillator. Under these conditions the energy of the vibronic states is given by<sup>15</sup>

$$E_\nu^n = \hbar\omega(N + n), \quad (20)$$

where  $N=1$  and  $\frac{3}{2}$  for the two- and three-dimensional problem, respectively,  $n$  is the vibronic quantum number, and  $\nu$  is the electronic quantum number corresponding to the specific manifold. An adequate oscillation wave function for the  $n$ th state can be presented by a linear combination of functions of the type

$$\chi_k^n(Q_1, Q_2) = \lambda^{n-k}(Q_1) \lambda^k(Q_2), \quad (21)$$

where  $k=0, 1, \dots, n$ , for the two-dimensional oscillator, and

$$\chi_{k,l}^n(Q_1, Q_2, Q_3) = \lambda^{n-k}(Q_1) \lambda^{k-l}(Q_2) \lambda^l(Q_3), \quad (22)$$

where  $k=0, 1, \dots, n$ ,  $l=0, 1, \dots, k$ , for the three-dimensional oscillator. In Eqs. (21) and (22),  $\lambda^m(Q)$  are the one-dimensional harmonic-oscillator wave functions. The density of states is

$$\rho(E^n) = (n+1)/\hbar\omega \quad (23)$$

and

$$\rho(E^n) = \sum_{n'=0}^n (n'+1)/\hbar\omega, \quad (24)$$

for a two- and three-dimensional oscillator, respectively.

To calculate the overlap integrals related to the vibronic wave functions of a "displaced" many-dimensional oscillator, one can choose the orthogonal coordinate sets in such a way that only one coordinate represents the "coupling" parallel mode  $Q_{\parallel}$ , whereas other coordinates correspond to perpendicular modes  $Q_{\perp}$  (see Fig. 2). Thus the functions (21) and (22) can be presented as follows:

$$\chi_k^n(Q_1, Q_2) = \lambda^{n-k}(Q_{\parallel}) \lambda^k(Q_{\perp}) \quad (25)$$

and

$$\chi_{k,l}^n(Q_1, Q_2, Q_3) = \lambda^{n-k}(Q_{\parallel}) \lambda^{k-l}(Q_{2\perp}) \lambda^l(Q_{3\perp}). \quad (26)$$

Since we have assumed the same phonon energies for all the modes involved,

$$\langle \lambda^n | \lambda^m \rangle_{\perp} = \delta_{nm}. \quad (27)$$

The procedure described above, i.e., the dividing of the modes into two classes depending on their properties, is very similar to the concept of promoting and accepting modes. Nevertheless, at this stage of the calculations, the

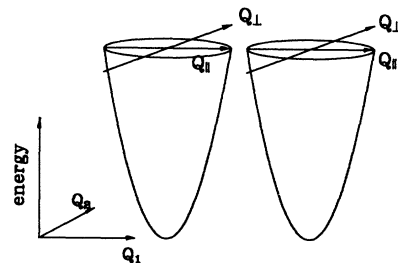


FIG. 2. Configuration-coordinate diagram for two two-dimensional harmonic oscillators. Parallel and perpendicular modes are shown in the  $Q_1, Q_2$  plane.

similarity is only formal, since parallel and perpendicular modes have been introduced for mathematical convenience. In the particular case when the  $H'$  is the electron-phonon interaction Hamiltonian given by Eq. (7), the parallel mode becomes a promoting mode and the perpendicular modes become accepting modes, in the sense of Refs. 4 and 5.

### C. Interaction with nonlocal lattice modes

The interaction of the electronic system with the nonlocal lattice vibrations usually does not cause the energy offset. Nevertheless, when the symmetry allows, this type of vibrations can produce an effective mixing of the electronic parts of the wave functions.

Let  $Q_{\text{latt}}$  be the configurational coordinate describing the nonlocal lattice distortion. We may define the perturbation Hamiltonian  $H'$  related to this type of distortion as follows:

$$H' = \frac{dV(q, Q_{\text{latt}})}{dQ_{\text{latt}}} Q_{\text{latt}}. \quad (28)$$

To consider the matrix elements of  $H'$  defined by Eq. (28), one should use the Born-Oppenheimer functions given by

$$\psi_v^m(q, Q, Q_{\text{latt}}) = \phi_v(q, Q) \chi_v^m(Q) \chi_v^N(Q_{\text{latt}}), \quad (29)$$

where  $\chi_v^N(Q_{\text{latt}})$  is the vibronic wave function describing the nonlocal mode. Since  $Q_{\text{latt}}$  can be represented by the sum of creation and annihilation operators (similar to the case of local modes), the matrix element of  $Q_{\text{latt}}$  is nonzero only when it connects the vibronic functions with  $N$  and  $N \pm 1$  vibronic quantum numbers.

Thus, in the frame work of our model,  $H'$  given by Eq. (28) can be treated as a purely electronic Hamiltonian; however, its matrix elements involving the functions (29) are additionally modified by a factor  $N^{1/2}$ , where  $N$  is the quantum number of the nonlocal lattice vibration state involved in the internal-conversion process.

### IV. TEMPERATURE DEPENDENCE OF INTERNAL-CONVERSION PROCESSES

One can consider the total probability of the internal conversion as a sum of transition probabilities related to all occupied vibronic states of the excited electronic manifold:

$$P_{\text{NR}}(T) = \sum_n \sum_{k(n)} W_{eg}^{(n,k)m} S^n, \quad (30)$$

where  $S^n$  is the Boltzmann distribution factor. In the above expression,  $n$  corresponds to the vibronic quantum number of the parallel mode and  $k$  corresponds to the vibronic quantum numbers of all perpendicular modes. Using this convention, we have no need to introduce the density of vibronic states in Eq. (30).

Considering Eqs. (25)–(27), one can obtain the  $P_{\text{NR}}(T)$  in more explicit form:

$$P_{\text{NR}}(T) = \tau_0^{-1} \sum_n \sum_{k=0}^n \delta(E_e^n - E_g^m) |F_{eg}^{n-k, m-k}|^2 \rho_k(E^n) S^n, \quad (31)$$

where

$$\tau_0^{-1} = (2\pi/\hbar)(\hbar\omega)^{-1} |\langle \phi_e | H'(q) | \phi_g \rangle|^2. \quad (32)$$

Here  $H'$  is the part of the perturbation Hamiltonian depending on the electronic coordinate only.  $F_{eg}^{n-k, m-k}$  is the overlap integral of parallel vibronic modes defined by Eq. (10) or (11) depending on the nature of the perturbation Hamiltonian.  $S^n$  is the Boltzmann occupation factor:

$$S^n = \exp[-(E_e^n - E_e^0)/kT] \times \left\{ \sum_n \exp[-(E_e^n - E_e^0)/kT] \rho(E^n) \right\}^{-1}. \quad (33)$$

$\rho(E^n)$  is the density of states and is equal to unity for a one-dimensional oscillator; for two and three dimensions,  $\rho$  is given by Eqs. (23) and (24), respectively.  $\rho_k(E^n)$  is the density of states of perpendicular modes and is equal to  $\delta_{k0}$ , 1, and  $(k+1)$  for the one-, two-, and three-dimensional oscillator, respectively.

One can immediately conclude that Eq. (31) can be reduced to the Struck-Fonger model for a one-dimensional oscillator when the Hamiltonian is purely electronic. In other cases our generalized approach yields a transition probability usually greater than the Struck-Fonger treatment.

### V. NONRADIATIVE DEEXCITATION OF Ti:SAPPHIRE

The  $\text{Ti}^{3+}$  ion in sapphire is an octahedrally coordinated  $d^1$  electron system. The crystal field yields the splitting of the  $d$  state into a doubly degenerate excited  ${}^2E$  state and triply degenerate  ${}^2T_2$  state (omitting the Kramers degeneracy).<sup>13</sup>

In spectroscopy, two bands in the absorption spectrum and one broadband in the emission spectrum are characteristic for a large static Jahn-Teller ( ${}^2E \times E$ ) and a small Jahn-Teller ( ${}^2T_2 \times E$ ) effect in the excited and ground states, respectively.<sup>16,9</sup> The detailed analysis of the spectroscopic data allows the reconstruction of the configuration-coordinate diagram of the system (see Fig. 3 in Ref. 17 and Fig. 4 in this work). It has been found that the electron-lattice coupling in the excited state is not linear. The value of the electron-phonon coupling constant  $K_E$  is in the range of 0.195C to 0.385C (C is the lattice elastic constant). On the other hand, the small second-order contribution to the electron-lattice coupling in the ground state ( $K_T = -0.077C$  to 0.077C) influences drastically the energy barrier for nonradiative transitions,  $E_{\text{NR}}$  (see Table IV in Ref. 17). Since this activation energy  $E_{\text{NR}}$  is not much greater than the difference between the energy of the minimum and the saddle point,  $\Delta_1$ , the excited-state electronic manifold can be represented by three two-dimensional harmonic oscillators (see Fig. 6 in Ref. 17). The calculated vibronic energies corresponding

to the excited state  $\hbar\omega_e$  are on order of  $200 \text{ cm}^{-1}$ .<sup>17,18</sup> The vibronic energy in the ground state is  $\hbar\omega_g=239 \text{ cm}^{-1}$ .<sup>19</sup> In all cases at the crossing point of the configuration-coordinate diagram (see Fig. 5 in Ref. 17 and Fig. 4 in this work), the lower component of the  ${}^2E$  state [ $\nu_{\pm 1/2}$  (Ref. (13))] is very effectively mixed with the upper component of the  ${}^2T_2$  state [ $\xi_{\pm 1/2}$  Ref. (13)], via the spin-orbit interaction. Therefore the spin-orbit interaction can be considered as a perturbation Hamiltonian of our system. The matrix elements of the perturbation potential  $H'$  are calculated as follows:

$$\langle \phi_e | H' | \phi_g \rangle = \langle \nu_{\pm 1/2} | H_{\text{s.o.}} | \xi_{\pm 1/2} \rangle = \pm i\beta, \quad (34)$$

where  $\beta$  is the spin-orbit crystal-field-theory parameter.<sup>13</sup>  $\beta=80 \text{ cm}^{-1}$  has been obtained in Ref. 17 by analysis of the spin-orbit splitting of the  ${}^2T_2$  state. Taking  $\hbar\omega=\hbar\omega_e=200 \text{ cm}^{-1}$  and using Eqs. (32) and (34), one can calculate the frequency factor  $\tau_0^{-1}$ :

$$\tau_0^{-1} \approx 3 \times 10^{13} \text{ s}^{-1}. \quad (35)$$

Since the symmetry conditions exclude the possibility of mixing the  ${}^2E$  and  ${}^2T_2$  states via the  $E$ -symmetry lattice distortion and there is no experimental evidence for large  $T_2$  distortion, one can consider the spin-orbit interaction as the only important contribution to the perturbation Hamiltonian. To calculate the vibronic overlap integrals which govern the internal-conversion transition probability, one divides the vibration into parallel and perpendicular modes. Considering two oscillators related to the  ${}^2E$  and  ${}^2T_2$  states, respectively, it can be seen that  $Q_\theta$  corresponds to the parallel and  $Q_\epsilon$  to the perpendicular vibration. Thus parallel oscillators are displaced by

$$\Delta Q_\parallel = |L_E/(1-K_E)| + |2L_T/(1+2K_T)|$$

and perpendicular ones by 0. Furthermore, since the energies of the vibrations in the ground and excited manifolds are different, Eq. (27) is not valid. This yields a more complicated expression for the internal-conversion probability, which includes the vibronic overlaps for the perpendicular mode:

$$P_{\text{NR}}(T) = \tau_0^{-1} \sum_n \sum_{k'=0}^m \sum_{k=0}^n \delta(E_e^n - E_g^m) |F_{eg}^{n-k, m-k'}|_\parallel^2 \times |F_{eg}^{kk'}|_\perp^2 S^n. \quad (36)$$

Here  $|F_{eg}^{n-k, m-k'}|_\parallel$  and  $|F_{eg}^{kk'}|_\perp$  are overlap integrals for parallel and perpendicular modes, respectively. Given that the perturbation Hamiltonian is purely electronic, the overlap integrals for both cases can be calculated according to Eq. (10).

To compare the results obtained using our approach with the experiment, we have reproduced the temperature dependence of fluorescence decay time for Ti:sapphire. It has been assumed that the total measured (effective) decay time  $\tau$  is controlled by the radiative as well as the nonradiative transition rates  $\tau_{\text{rad}}^{-1}$  and  $\tau_{\text{NR}}^{-1}$ . Thus

$$\tau = (\tau_{\text{rad}}^{-1} + \tau_{\text{NR}}^{-1})^{-1}. \quad (37)$$

The radiative decay time has been assumed to be equal to the measured decay in the limit of zero temperature, and so  $\tau_{\text{rad}}=3.85 \text{ }\mu\text{s}$ .<sup>17</sup> The nonradiative transition rate has been calculated assuming that the internal conversion is the only nonradiative process depopulating the  ${}^2E$  state, i.e.,  $\tau_{\text{NR}}^{-1}=P_{\text{NR}}(T)$  [Eq. (36) with  $\tau_0^{-1}$  given by Eq. (35)]. The vibronic overlap integrals for individual pairs of the vibronic wave functions have been calculated using the Manneback recurrence approach.<sup>20</sup> The results of the calculations, with a comparison to the experimental results of Albers, Stark, and Huber<sup>9</sup> and Moulton,<sup>21</sup> are presented in Fig. 3. The dashed curves have been obtained using the value of  $\tau_0^{-1}=3 \times 10^{13} \text{ s}^{-1}$  and the parameters of configurational energy manifolds listed in Table IV of Ref. 17: curve I corresponds to  $K_T=0$ ,  $K_E=0.289$ ,  $E_{\text{JT}}(E)=2909 \text{ cm}^{-1}$ ,  $E_{\text{JT}}(T)=158 \text{ cm}^{-1}$ , and curve II corresponds to  $K_T=-0.077$ ,  $K_E=0.195$ ,  $E_{\text{JT}}(E)=2993 \text{ cm}^{-1}$ ,  $E_{\text{JT}}(T)=113 \text{ cm}^{-1}$ . If one uses a third parameter set to reproduce the spectroscopic data [ $K_T=0.077$ ,  $K_E=0.385$ ,  $E_{\text{JT}}(E)=2879 \text{ cm}^{-1}$ ,  $E_{\text{JT}}(T)=223 \text{ cm}^{-1}$ ], with  $\tau_0^{-1}$  given by Eq. (35), the calculated decay is approximately two orders of magnitude smaller than measured. In this case the very low nonradiative activation energy ( $E_{\text{NR}}=985 \text{ cm}^{-1}$ ) yields large values of the overlap integrals. For instance, the overlap corresponding to the zero vibration state of the  ${}^2E$  manifold,  $|F_{eg}^{00}|^2$ , is on the order of  $10^{-5}$ . Since the experimental decays are placed between the theoretical decays obtained for the limiting values of  $K_T$ , we may treat  $K_T$  as a free parameter for fitting purposes. The best fit has

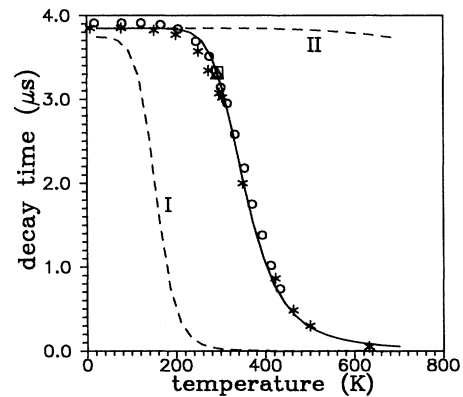


FIG. 3. Luminescence decay time for Ti:sapphire vs temperature. Dashed curves correspond to the sets of the input parameters of configuration-coordinate diagrams as follows: I corresponds to  $K_T=0$ ,  $K_E=0.289$ ,  $E_{\text{JT}}(E)=2909 \text{ cm}^{-1}$ ,  $E_{\text{JT}}(T)=158 \text{ cm}^{-1}$  ( $E_{\text{NR}}=2633 \text{ cm}^{-1}$ ); II corresponds to  $K_T=-0.077$ ,  $K_E=0.195$ ,  $E_{\text{JT}}(E)=2993 \text{ cm}^{-1}$ ,  $E_{\text{JT}}(T)=113 \text{ cm}^{-1}$  ( $E_{\text{NR}}=7171 \text{ cm}^{-1}$ ) (see Ref. 17). The solid curve corresponds to the best fit. Asterisks correspond to the experimental data by Albers, Stark, and Huber (Ref. 9); circles correspond to the experimental data of Moulton (Ref. 21).  $\square$  corresponds to our annealed sample;  $\triangle$  corresponds to our normal sample (Ref. 17).

TABLE I. Parameters of configuration-coordinate diagram for the best fit  $K_T = -0.043$ .

$K_E$	$E_{JT}(E)$	$E_{JT}(T)$	$\hbar\Omega_4$ ( $\text{cm}^{-1}$ )	$\hbar\omega_{e1}$	$\hbar\omega_{e2}$	$E_{NR}$	$\Delta_1$
0.236	2924	132	11 225	208	202	4507	1125

been obtained for  $K_T = -0.043C$  (solid curve in Fig. 3). The calculations have been performed considering that the resulting electronic manifolds should reproduce also the spectroscopic data (see Ref. 17). This induces a small change in the values of other parameters defining the system; see Table I. The respective configuration-coordinate diagram is presented in Fig. 4.

To compare our results with the Struck-Fonger model, we have performed a calculation of the vibronic overlap-integral quenching factor resulting from our model:

$$f(n) = \sum_{k'=0}^m \sum_{k=0}^n \delta(E_e^n - E_g^m) |F_{eg}^{n-k, m-k'}|^2 |F_{eg}^{kk'}|^2 \quad (38)$$

and of the respective Struck-Fonger overlap integral

$$F_{SF}(n) = \delta(E_e^n - E_g^m) |F_{eg}^{nm}|^2, \quad (39)$$

which can be obtained from Eq. (38) assuming

$$F_{eg}^{kk'} = \delta_{kk'} \quad (40)$$

and

$$\sum_{k=0}^n |F_{eg}^{n-k, m-k}|^2 = |F_{eg}^{nm}|^2. \quad (41)$$

Since  $|F_{eg}^{ij}|$  rapidly increases with increasing  $i$  and  $j$  and the vibronic energies related to the excited and the ground manifolds do not differ much, the above approximations seem to be reasonable. The results of the calculations are presented in Fig. 5. Asterisks correspond to the overlap-integral quenching factor calculated accord-

ing to our Eq. (38), and circles correspond to the simplified approach [Eq. (39)]. Lines connecting the points have been added to aid the eye. One can see that for the assumed values of input parameters [ $K_T = -0.043$ ,  $K_E = 0.236$ ,  $E_{JT}(E) = 2924 \text{ cm}^{-1}$ ,  $E_{JT}(T) = 132 \text{ cm}^{-1}$ ] the Struck-Fonger approach is still a reasonable approximation, although it gives smaller values of the overlap integrals.

The quantitative results presented in this section have been obtained under the assumption that the spin-orbit interaction is the only interaction which is responsible for the internal conversion process in  $\text{Ti}^{3+}$ . Thus only the value of the parameter  $\beta$  determines the frequency factor  $\tau_0^{-1}$ . Assuming that additional mechanisms allowing the internal conversion are possible (the interaction with  $T_2$ -symmetry lattice distortion and interaction with nonlocal lattice vibrations), we can see that the value of  $\tau_0^{-1}$  used may be underestimated. An increased frequency factor above  $3 \times 10^{13} \text{ s}^{-1}$  may be easily compensated for by smaller overlap integrals, which rapidly decrease with a decreasing value of  $K_T$ . In fact, these two parameters,  $\tau_0^{-1}$  and  $K_T$ , are closely related to each other. On the other hand, the values of the remaining parameters describing the system ( $K_E, E_{JT}(E), E_{JT}(T)$ ) are almost the same, since they are determined mainly by the spectroscopic data (see Table IV in Ref. 17 and Table I in this work). Only the nonradiative activation energy  $E_{NR}$  effectively increases with decreasing  $K_T$ . Thus one concludes that since the value of  $\tau_0^{-1} = 3 \times 10^{13} \text{ s}^{-1}$  is the lower-limit value, the nonradiative transition activation energy  $E_{NR} = 4507 \text{ cm}^{-1}$  is also the lower-limit value for  $\text{Ti}^{3+}:\text{Al}_2\text{O}_3$ . The remaining parameters of the configuration-coordinate diagram seem to be estimated quite accurately.

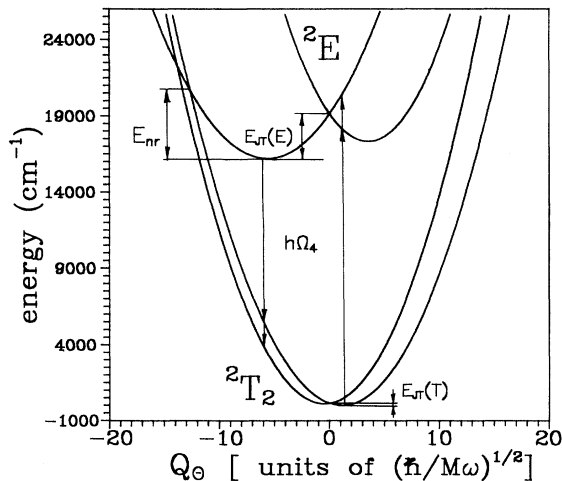


FIG. 4. Configuration-coordinate diagram for  $\text{Ti}^{3+}$ :sapphire, cross-section direction. Intersystem crossing is not discontinuous, since the diagram has been calculated in the diabatic limit.

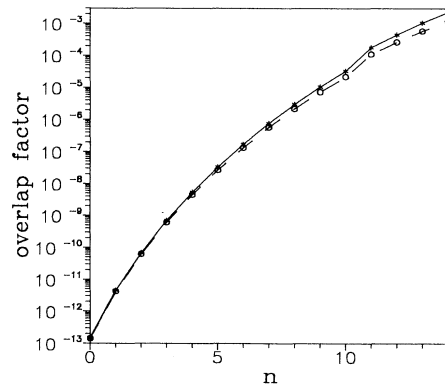


FIG. 5. Vibronic overlap-integral reduction factor vs excitation vibronic number  $n$ . The solid curve corresponds to the calculations performed for the two-dimensional case [Eq. (38)]; the dashed curve corresponds to the Struck-Fonger formula [Eq. (39)].

## VI. CONCLUSIONS

Both the adiabatic and diabatic approaches have been examined with respect to the perturbation Hamiltonian which induces nonradiative deexcitations of transition-metal ions in solids. The methodologies were further applied to the  $\text{Ti}^{3+}:\text{Al}_2\text{O}_3$  system and were found to describe successfully the temperature quenching of  $\text{Ti}^{3+}:\text{sapphire}$  luminescence, including the observed luminescence decay times reported in the literature and those from our samples. The theoretical nonradiative transition rate was calculated under the assumption that the spin-orbit interaction is the only process responsible for the internal-conversion rate in  $\text{Ti}^{3+}$ . The expressions for the nonradiative transition rate involve a generalized vibronic overlap-integral quenching factor, which, in special cases, yields the well-known Struck-Fonger overlap integral. The values of the nonradiative rates obtained in the present generalized theoretical nonradiative framework were found to be in closer quantitative correspondence to the experimental values than the Struck-Fonger approach.

## APPENDIX: DIABATIC AND ADIABATIC APPROACHES TO A TRANSITION-METAL CONFIGURATION ENERGY MANIFOLD

In the most general case, the system of an electron (or electrons) interacting with the lattice ions can be described by the following Hamiltonian:

$$H = H_e(q, Q) - \frac{1}{2} \nabla_Q^2, \quad (\text{A1})$$

where  $H_e(q, Q)$  is the electronic part of the Hamiltonian depending on the electronic ( $q$ ) and ionic ( $Q$ ) coordinates, and  $\frac{1}{2} \nabla_Q^2$  is the lattice kinetic energy. For simplicity, the ionic coordinate  $Q$  is given in  $(\hbar/M\omega)^{1/2}$  units, where  $\omega$  is the frequency of the lattice vibration and  $M$  is the reduced mass of the involved ions.

In the Born-Oppenheimer approximation, being in the  $n$ th electronic and  $m$ th vibronic state, the system is described by the total wave function  $\psi_n^m$ ,

$$\psi_n^m = \phi_n(q, Q) \chi_n^m(Q), \quad (\text{A2})$$

where  $\phi$  and  $\chi$  correspond to electronic and vibronic parts of the wave function. Since the Hamiltonian (A1) is separable in the variables  $q$  and  $Q$ , one can obtain  $Q$ -dependent configurational energies by diagonalization of the electronic part of the Hamiltonian  $H_e$ . This procedure creates the adiabatic electronic wave functions  $\phi^a(q, Q)$ , for which

$$\langle \phi_i^a | H_e | \phi_j^a \rangle = \epsilon_j(Q) \delta_{ij}. \quad (\text{A3})$$

Here  $\langle \dots \rangle$  denotes an integration over the  $q$  coordinate.

Using (A3), one obtains the set of equations defining the adiabatic vibronic states of the system:

$$\left\{ -\frac{1}{2} \nabla_Q^2 \mathbf{I} - \epsilon(Q) - E \mathbf{I} + \frac{1}{2} [2 \mathbf{A}(Q) \nabla_Q + \mathbf{B}(Q)] \right\} \chi^a(Q) = 0. \quad (\text{A4})$$

Here  $\mathbf{I}$  is the unit matrix and  $\epsilon(Q)$  is diagonal matrix.  $\mathbf{A}(Q)$  and  $\mathbf{B}(Q)$  are matrices with the elements

$$\begin{aligned} A_{ij} &= \langle \phi_i^a | \nabla_Q | \phi_j^a \rangle, \\ B_{ij} &= \langle \phi_i^a | \nabla_Q^2 | \phi_j^a \rangle. \end{aligned} \quad (\text{A5})$$

$\chi^a(Q)$  represent the set of vibronic, adiabatic wave functions. When the adiabatic base is complete,<sup>22</sup>

$$\mathbf{B} = \mathbf{A}^2 + \nabla_Q \mathbf{A}. \quad (\text{A6})$$

One may obtain the approximate solutions of (A4) by omitting  $\mathbf{A}$  and  $\mathbf{B}$  as small. Here such an approximation has been made, to define the adiabatic vibronic states related to the individual manifolds described by  $\epsilon_i(Q)$  and  $\phi_i^a(q, Q)$ . In fact,

$$\frac{1}{2} [2 \mathbf{A}(Q) \nabla_Q + \mathbf{B}(Q)] = \mathbf{H}_{\text{NA}} \quad (\text{A7})$$

is the so-called nonadiabatic operator [see also Eq. (3) in the main text]. The matrix  $\mathbf{H}_{\text{NA}}$  is off diagonal, and therefore it is responsible for the mixing of the vibrational states related to different electronic manifolds.

We can now define a "diabatic"<sup>23</sup> set of nuclear wave functions as follows:

$$\chi^a(q, Q) = G(Q) \chi^d(q, Q), \quad (\text{A8})$$

where the matrix  $\mathbf{G}$  is any matrix which satisfies the relationship<sup>23</sup>

$$\frac{d\mathbf{G}(Q)}{dQ} + \mathbf{A}(Q)\mathbf{G}(Q) = 0. \quad (\text{A9})$$

Then, using (A7) and (A9), one transforms (A4) into the form

$$\left\{ -\frac{1}{2} \nabla_Q^2 \mathbf{I} - \mathbf{V}(Q) - E \mathbf{I} \right\} \chi^d(Q) = 0. \quad (\text{A10})$$

Here

$$\mathbf{V}(Q) = \mathbf{G}^{-1}(Q) \epsilon(Q) \mathbf{G}(Q). \quad (\text{A11})$$

One can see that the diabatic and adiabatic electronic wave functions are related by

$$\phi^d(q, Q) = \phi^a(q, Q) \mathbf{G}(Q). \quad (\text{A12})$$

It is obvious that, for any  $i$  and  $j$ ,<sup>23</sup>

$$\langle \phi_i^d | \nabla_Q | \phi_j^d \rangle = 0. \quad (\text{A13})$$

The above calculation can be exemplified when we consider the transition-metal system which can be described by two electronic manifolds: the excited  $e$  and the ground  $g$  manifold. In this case one can use the crystal-field-approximation electronic wave functions  $\phi_e(q) = \phi_e(q, Q_0)$  and  $\phi_g(q) = \phi_g(q, Q_0)$  as an initial basis. By definition, these functions do not depend on the configuration coordinate  $Q$ , since the crystal-field Hamiltonian has been taken with the ions fixed at  $Q_0$  ( $Q_0$  defines the crystal-field strength). To focus our attention, we can assume that  $Q_0$  corresponds to the minimum energy of the ground electronic manifold. Thus, putting  $Q_0 = 0$ , one can obtain the electronic energies  $\epsilon(Q)$  in the adiabatic limit (the configurational energy manifolds in



the adiabatic limit) from the determinantal equation

$$\begin{vmatrix} Q^2/2 - \epsilon(Q) & H'(Q) \\ H'(Q) & Q^2/2 + (2S)^{1/2}Q + \Delta E + S - \epsilon(Q) \end{vmatrix} = 0. \quad (\text{A14})$$

Here  $(2S)^{1/2}Q$  is the diagonal part of the electron-lattice interaction Hamiltonian ( $S$  is the Huang-Rhys parameter);  $\Delta E$  is  $e-g$  separation energy; and  $H'$  is the part of the Hamiltonian which mixes the ground and excited state wave functions. Depending on the system,  $H'$  may be the matrix element of spin-orbit interaction or a part

of electron-phonon interaction. One obtains the energies:

$$\epsilon_{\pm}(Q) = \frac{1}{2} (Q^2(2S)^{1/2}Q + \Delta E + S \pm \{[(2S)^{1/2}Q + \Delta E + S]^2 + 4H'^2\}^{1/2}). \quad (\text{A15})$$

The adiabatic wave functions  $\phi^a(q, Q)$  describing the electronic manifolds  $\epsilon_{\pm}(Q)$  are related to the initial basis wave function by the matrix  $\mathbf{d}$ ,

$$\phi^a(q, Q) = \mathbf{d}(Q)\phi(q), \quad (\text{A16})$$

which for our case can be easily obtained:

$$\begin{aligned} d_{1e}(Q) &= d_{2g}(Q) = 2^{-1/2} (1 + [(2S)^{1/2}Q + \Delta E + S] / \{[(2S)^{1/2}Q + \Delta E + S]^2 + 4H'^2\}^{1/2}), \\ d_{2e}(Q) &= -d_{1g}(Q) = 2^{-1/2} (1 - [(2S)^{1/2}Q + \Delta E + S] / \{[(2S)^{1/2}Q + \Delta E + S]^2 + 4H'^2\}^{1/2}). \end{aligned} \quad (\text{A17})$$

The electronic configuration manifolds in the adiabatic limit,  $\epsilon_+(Q)$  and  $\epsilon_-(Q)$ , are presented in Fig. 1(a). One can obtain the vibronic state of the system using Eq. (A4), where the matrix elements of  $\mathbf{A}$  and  $\mathbf{B}$  can be calculated using Eq. (A16). As a first approximation, one can obtain the vibronic states for individual manifolds, assuming  $\mathbf{H}_{\text{NA}} = 0$ . Next  $\mathbf{H}_{\text{NA}}$  can be treated in the framework of the perturbation approach to obtain more exact solutions. However, even under this simplification, the problem is difficult since the vibronic problem must be solved for quite a general potential. Since the perturbation Hamiltonian is always  $\mathbf{H}_{\text{NA}}$ , one can see that in the adiabatic limit all information on the physical reasons of the interconfigurational interactions is contained in the particular shape of configurational energies and adiabatic electronic wave functions.

It is easy to prove that  $\mathbf{d}^{-1} = \mathbf{G}$ , since the matrix  $\mathbf{d}^{-1}$  satisfies the relation [corresponding to Eq. (A9)]

$$\frac{\partial(\mathbf{d}^{-1}(Q))}{\partial Q} - \mathbf{A}(Q)\mathbf{d}^{-1}(Q) = 0. \quad (\text{A18})$$

One can check Eq. (A18) using relations (A17) and adiabatic functions (A16) to obtain the matrix  $\mathbf{A}$ . In such cases the initial basis of the electronic functions  $\phi_e(q)$  and  $\phi_g(q)$  creates the diabatic basis of the system. In Eq. (A18) the operator  $\partial/\partial Q$  instead of  $d/dQ$  has been used to avoid misunderstanding when the same symbol describes the function and the derivative operator. In this manner the vibrational problem in the diabatic representation can be described by the Hamiltonian

$$\begin{vmatrix} \frac{1}{2}\nabla_Q^2 + Q^2/2 - E & H'(Q) \\ H'(Q) & -\frac{1}{2}\nabla_Q^2 + Q^2/2 + (2S)^{1/2}Q + \Delta E + S - E \end{vmatrix} \begin{bmatrix} \chi_e^d(Q) \\ \chi_g^d(Q) \end{bmatrix} = 0. \quad (\text{A19})$$

Here the diagonal elements correspond to the diabatic manifolds presented in Fig. 1(b). Similar to the adiabatic approximation, one can use the perturbation method and, as a first approximation, assume  $H' = 0$ . One can see immediately that, since the electronic energies in both manifolds are given by parabolas, the vibronic problem is reduced to the harmonic oscillator. Moreover, since the initial basis has been defined for constant  $Q_0$ , performing calculations in the diabatic limit, one operates with electronic wave functions not dependent on the configurational coordinate. One can see that for all cases when the crystal-field base is adequate to describe the system, the problem of finding the diabatic base is, in fact, trivial.

<sup>1</sup>N. F. Mott, Proc. R. Soc. London A **167**, 384 (1938).

<sup>2</sup>C. W. Struck and W. H. Fonger, J. Lumin. **10**, 1 (1975).

<sup>3</sup>W. H. Fonger and C. W. Struck, Phys. Rev. B **11**, 3251 (1975).

<sup>4</sup>R. H. Bartram and A. M. Stoneham, J. Phys. C **18**, L49 (1985).

<sup>5</sup>R. H. Bartram, J. C. Charpie, L. J. Andrews, and A. Lempicki, Phys. Rev. B **34**, 2741 (1986).

<sup>6</sup>R. Englman, *Non-Radiative Decay of Ions and Molecules in Solids* (North-Holland, Amsterdam, 1979).

<sup>7</sup>Cz. Koepke, A. Lempicki, and G. H. Beall, J. Lumin. (to be published).

<sup>8</sup>Li-Ji Lyu and D. S. Hamilton, J. Lumin. **48&49**, 251 (1991).

<sup>9</sup>P. Albers, E. Stark, and G. Huber, J. Opt. Soc. Am. B **3**, 134 (1986).

<sup>10</sup>G. W. Robinson and R. P. Frosch, J. Chem. Phys. **37**, 1962; **38**, 1187 (1963).

<sup>11</sup>K. F. Freed, in *Radiationless Processes in Molecular and Con-*

- densed Phases*, edited by F. K. Fong (Springer-Verlag, Heidelberg, 1976).
- <sup>12</sup>A. S. Davydov, *Quantum Mechanics* (Nauka, Moscow, 1963).
- <sup>13</sup>See, for instance, Y. Tanabe, S. Sugano, and H. Kamimura, *Multiplets of Transition Metal Ions in Crystals* (Academic, New York, 1970).
- <sup>14</sup>M. D. Sturge, *Phys. Rev. B* **8**, 6 (1973).
- <sup>15</sup>C. Cohen-Tannoudji, B. Diu, and F. Laloe, *Quantum Mechanics* (Wiley-Interscience, New York, 1977), Vol. I.
- <sup>16</sup>R. M. MacFarlane, J. T. Wong, and M. D. Sturge, *Phys. Rev.* **166**, 250 (1968); L. Cianchi, M. Mancini, and P. Moretti, *Phys. Rev. B* **7**, 5014 (1973); C. E. Byvik and M. Buoncrisiani, *IEEE J. Quantum Electron.* **QE-21**, 1619 (1985).
- <sup>17</sup>M. Grinberg, A. Mandelis, K. Fjelsted, and A. Othonos, the preceding paper, *Phys. Rev. B* **48**, 5922 (1993).
- <sup>18</sup>R. Englman, *The Jahn-Teller Effect in Molecules and Crystals* (Wiley-Interscience, New York, 1972).
- <sup>19</sup>B. F. Gachter and J. A. Koningstein, *J. Chem. Phys.* **60**, 2003 (1974).
- <sup>20</sup>C. Manneback, *Physica* **17**, 1001 (1951).
- <sup>21</sup>P. F. Moulton, *J. Opt. Soc. Am. B* **3**, 125 (1986).
- <sup>22</sup>F. T. Smith, *Phys. Rev.* **179**, 111 (1969).
- <sup>23</sup>T. G. Heil and A. Dalgarno, *J. Phys. B* **12**, L557 (1979); T. G. Heil, S. E. Butler, and A. Dalgarno, *Phys. Rev. A* **23**, 1100 (1981).